Cell Research (2012) 22:777-781.

www.nature.com/cr

LETTER TO THE EDITOR

F-box protein AFB4 plays a crucial role in plant growth, development and innate immunity

Cell Research (2012) **22**:777-781. doi:10.1038/cr.2012.12; published online 17 January 2012

Dear Editor,

Auxin-signaling F-box protein 4 (AFB4) encoded by At4g24390 shares a significant sequence similarity to auxin receptor TIR1. In this study, we used a combination of physiological, molecular, and genetic approaches to characterize a T-DNA insertion line (GABI-KAT accession no.: 068E01; henceforth designated *afb4-1*) as a knockout allele. Complete loss-of-function of the *AFB4* gene confers defects in many aspects of the plant life cycle including lateral root development, hypocotyl elongation, leaf organogenesis, flowering time, seed formation, and disease resistance to specific phytopathogens. The results presented here argue against the previously proposed mechanism of AFB4 action in negatively controlling auxin sensitivity [1].

afb4-1 mutants showed a pleiotropic phenotype. One of the most conspicuous features is that *afb4-1* displayed extremely small but distorted rosette leaves with short petiole (Figure 1A and 1B). A closer examination of fully expanded leaves under a light microscope disclosed similar epidermal cells without size alternation in *afb4-1* compared with wild-type (WT) plants, whereas leaf thickness was increased (Supplementary information, Figure S1). In accordance with the latter observation, the final cell volume of leaf blades in *afb4-1* was significantly larger than that in WT, which probably compensates for the defect in the final size of leaf blades to some extent, as observed in many leaf mutants [2]. By contrast, a drastic decrease in the length of petiole cells (Figure 1C) certainly accounts for the markedly reduced elongation of *afb4-1* petiole (Figure 1B). Unlike *afb4-2* and *afb4-3* [1], inspection of WT and mutant primary root growth failed to uncover any statistical difference (Figure 1D). However, *afb4-1* seedlings had less lateral roots protruding from primary roots (Figure 1D), indicating that AFB4 might be involved in activation of a lateral root development program. Moreover, the requirement of AFB4 for hypocotyl elongation is evident from the observation that seedlings exhibited substantially shorter hypocotyls (Figure 1D). Besides the obvious changes in lateral root growth and leaf organogenesis, *afb4-1* was easily distinguishable from WT in terms of distinct morphological traits, including a great decrease in plant height (Figure 1E), and a noticeable delay in the transition from the vegetative to the reproductive stage (Figure 1F). Despite a pronounced reduction in size, weight, and yield of seeds (Figure 1G and 1H), the viability was not affected, suggesting a normal embryo development in *afb4-1*. Indeed, no defect was detected at different developmental stages of *afb4-1* embryogenesis (Supplementary information, Figure S2).

Since growth and development of plant organs are largely governed by phytohormones [3], we asked if hormone-mediated responses are modified in *afb4-1*. Responsiveness to various hormones over a wide range of concentrations was quantified by physiological assays for inhibition of primary root growth or for stimulation of hypocotyl elongation (Supplementary information, Figure S3). Apparently, *afb4-1* showed altered sensitivity to exogenous application of 1-aminocyclopropane-1-carboxylic acid (a natural precursor of ethylene), 24-epibrassinolide, gibberellins A_3, and abscisic acid. These results implicate AFB4 proteins as important participants in multiple hormonal signaling pathways. On the other hand, *afb4-1* did not differ substantially from WT upon treatments with indole acetic acid (IAA), kinetin, and trans-zeatin, suggesting an intact auxin or cytokinin signaling in *afb4-1*.

Emerging evidence pinpoints that auxin-dependent processes are regulated in a tissue-specific manner, [4, 5] and a short hypocotyl is characteristic of auxin-response *aux/iaa* mutants [6], prompting us to speculate that a hypocotyl-specific auxin-code might be changed in *afb4-1*. In support of the hypothesis, IAA induction of the auxin-signaling marker *IAA5* was partially diminished (Figure 1I). Furthermore, auxin-dependent induction of hypocotyl elongation under high temperature [7] appeared to be impaired (Figure 1J). Although it is not yet known if T-DNA disturbance causes an inhibitory effect on high-temperature-induced auxin production or a signal transduction defect responding to auxin in *afb4-1*, our data

highlight the requirement of functional AFB4 for auxin-mediated growth response of hypocotyl elongation.

Given the various defects in growth and development, we wondered if T-DNA interruption of *AFB4* might result in adverse effects on plant's immunity. Interestingly, *afb4-1* showed enhanced resistance following challenge with a virulent strain SCC1 of *Pectobacterium carotovorium* subsp. *carotovorum* [8]. In sharp contrast to the massively spreading maceration in WT, disease symptom was strongly attenuated in *afb4-1* with a limited maceration accompanied by necrotic lesion in inoculated leaves (Figure 1K). Consistent with this observation, bacterial growth *in planta* was dramatically reduced (Figure 1K). These results indicate that elimination of the *AFB4* gene directly contributes to reduced susceptibility of *afb4-1* to SCC1.

To firmly establish the causal link between *AFB4* and the observed phenotypes, we carried out molecular genetic analyses. Confirmation of the insertion via a PCR-based approach was followed by DNA sequencing (Supplementary information, Figure S4A and S4B). As predicted, no full-length transcript was detected in homozygous *afb4-1* (Figure S4C). However, the T-DNA insertion led to an abnormal transcript in both heterozygotes and homozygotes (Supplementary information, Figure S4D). The cDNA derived from aberrant mRNAs predicted a truncated protein (Supplementary information, Figure S4E). Furthermore, co-segregation analyses (Supplementary information, Figure S4F) suggest that growth defects are tightly associated with the defined T-DNA. Notably, a semidominant growth phenotype in heterozygotes raised the possibility that truncated proteins in heterozygotes compete with normal AFB4 and thus confers a dominant negative property. To rule out this, we generated overexpression lines in WT background, which exactly harbored the same artificial gene as present in *afb4-1* but driven by CaMV-35S. All lines displayed a WT phenotype even if with robust overexpression (Supplementary information, Figure S5), indicative of a non-functional truncated *afb4-1* protein. To further clarify that the intermediate phenotype in heterozygotes results from reduced levels in *AFB4* transcripts, we modulated endogenous contents of *AFB4* mRNAs via antisense-mediated gene silencing. Representatives were shown with a great deal

Figure 1 Functional analysis of the *AFB4* gene in *Arabidopsis thaliana*. **(A)** Morphology of 12-day-old *afb4-1* seedlings grown in ½MS liquid medium. **(B)** Leaf organogenesis in *afb4-1* homozygotes. The fifth leaves from 28-day-old soil-grown plants were photographed. **(C)** Comparison of petiole cells in WT and *afb4-1* plants under a light microscopy. **(D)** Roots and hypocotyls of *afb4-1*. The length of primary roots and hypocotyls was measured with 7-day-old seedlings, whereas 14-day-old seedlings were used for counting the lateral roots. The means and standard deviations were calculated from 30 individuals. The seedling growth assay was independently repeated three times with similar results. **(E)** Height of 56-day-old soil-grown plants. The means and standard deviations were calculated from 28 individual plants. The experiments were independently performed twice with similar results. **(F)** Flowering time among different genotypes. Error bars indicate the standard deviation of 28 plants. Similar results were obtained from two independent experiments. **(G)** Comparison of seed weight. Error bars for seed weight indicate the standard deviation of three random measurements with 1 000 seeds per genotype. **(H)** Seed yield. Plants were fertilized three times during the whole life cycle. Seeds derived from 10 individual plants were pooled as one sample. The error bars represent standard deviation of three samples. Two independent experiments were carried out with similar results. **(I)** Auxin-induction of the *IAA5* gene in different genotypes. For each sample, ~100 seedlings at a 9-day-old stage were used. Data are shown as means ± standard errors from three independent biological replicates using the mock treatment (H_2O) as the control of 2 μM IAA at the indicated time points. **(J)** Temperature-induced hypocotyl elongation growth response. *tir1-1* mutants were used as a negative control. Hypocotyls were measured from 9-day-old seedlings of WT, *afb4-1*, and *afb4-1* transgenic lines harboring the full-length cDNA of *AFB4* under control of the 35S promoter. Data represent the mean measurement of 30 individual seedlings. Error bars indicate standard deviation. Similar results were obtained from two independent experiments. **(K)** Pathogen infection. Inoculation was performed with the virulent strain SCC1 of *Pectobacterium carotovorium* subsp. *carotovorium* at 1×10^5 cfu/ml. Each sample consisted of eight individual plants. Data are shown as means ± standard errors from three biological replicates. **(L)** Morphology of independent antisense-silenced *afb4* alleles at 21-day-old stage. **(M)** The relative expression levels of *AFB4* transcripts in the corresponding lines **(L)** by RT-qPCR analyses. Data are shown as means ± standard errors. ND: not detectable. **(N)** *AFB4* overexpressors in *afb4-1* background. Images show 28-day-old representatives from two independent overexpression lines in comparison to WT. **(O)** Genetic complementation. 28-Day-old transgenic plants, which possessed the *AFB4* cDNA under the control of the 35S promoter in *afb4-1* background, showed the full restoration of growth morphology. **(P)** The relative expression levels of *AFB4* mRNAs in independent transgenic lines bearing the *AFB4* cDNA under the control of the 35S promoter. Data are shown as means ± standard errors from three independent biological replicates. **(Q)** Petiole length of 9-day-old *afb4-2* and *afb4-3* seedlings (*AFB4-afb4-2* or *AFB4-afb4-3*) in comparison to the transgenic lines carrying the intact *AFB4* locus (*AFB4-AFB4*) or its full-length cDNA driven by the 35S promoter **(***H3* or *H15* corresponding to two lines described in **N** in *afb4-1* background. Each sample consisted of 30 seedlings. Data are shown as means ± standard errors from three independent biological replicates.

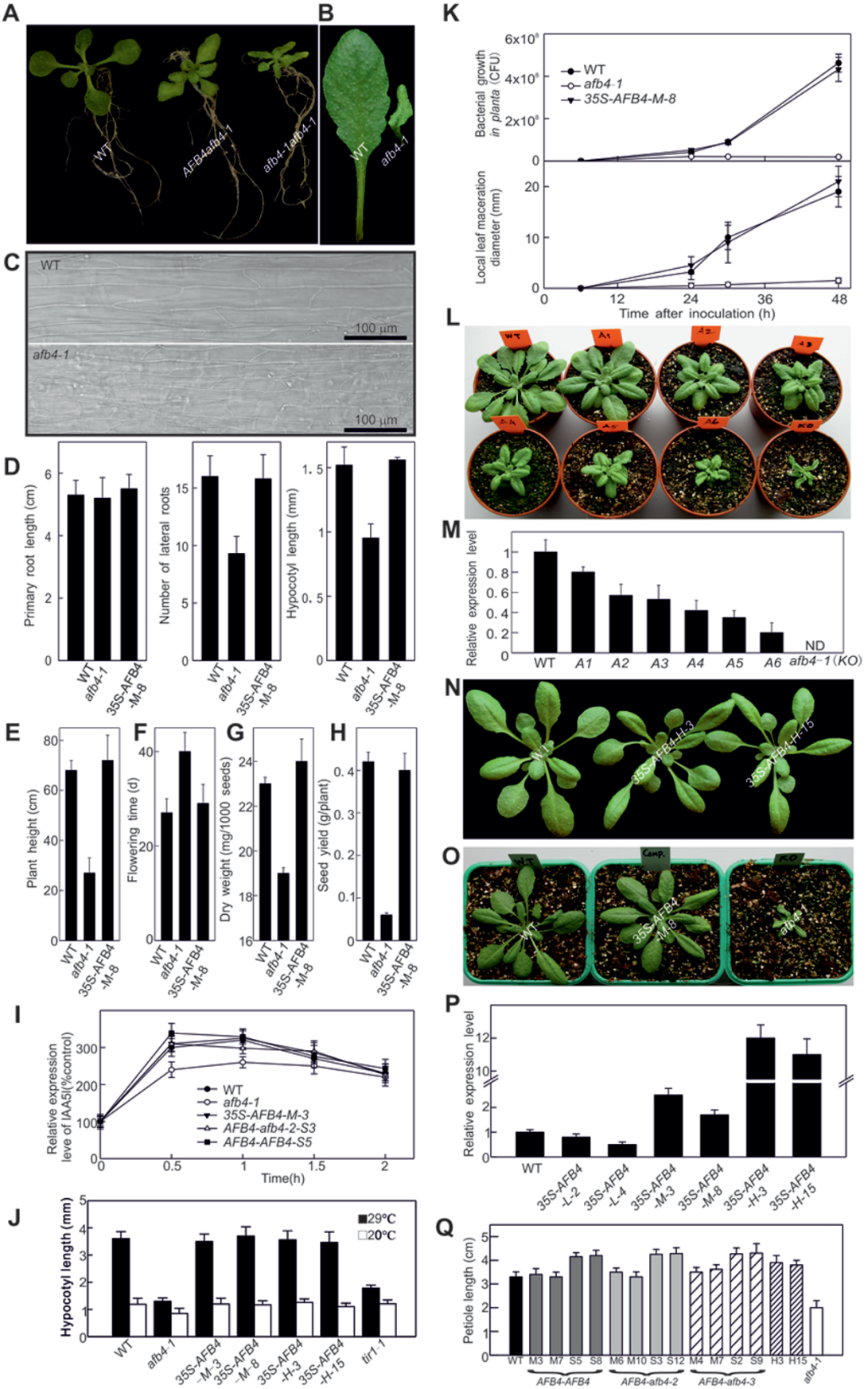
A
WT
AFB4-afb4-1
afb4-1-afb4-1
B
WT
afb4-1
C
WT
100 μm
afb4-1
100 μm
D
Primary root length (cm)
Number of lateral roots
Hypocotyl length (mm)
WT
afb4-1
35S-AFB4 -M-8
E
Plant height (cm)
F
Flowering time (d)
G
Dry weight (mg/1000 seeds)
H
Seed yield (g/plant)
I
Relative expression leve of IAA5l(%control)
Time(h)
WT
afb4-1
35S-AFB4-M-3
AFB4-afb4-2-S3
AFB4-AFB4-S5
J
Hypocotyl length (mm)
29°C
20°C
WT
afb4-1
35S-AFB4 -M-3
35S-AFB4 -M-8
35S-AFB4 -H-3
35S-AFB4 -H-15
tir1-1
K
Bacterial growth in planta (CFU)
WT
afb4-1
35S-AFB4-M-8
Local leaf maceration diameter (mm)
Time after inoculation (h)
L
M
Relative expression level
WT
A1
A2
A3
A4
A5
A6
afb4-1(KO)
ND
N
WT
35S-AFB4-H-3
35S-AFB4-H-15
O
WT
Comp.
KO
35S-AFB4 -M-8
afb4-1
P
Relative expression level
WT
35S-AFB4 -L-2
35S-AFB4 -L-4
35S-AFB4 -M-3
35S-AFB4 -M-8
35S-AFB4 -H-3
35S-AFB4 -H-15
Q
Petiole length (cm)
WT M3 M7 S5 S8 M6 M10 S3 S12 M4 M7 S2 S9 H3 H15 afb4-1
AFB4-AFB4
AFB4-afb4-2
AFB4-afb4-3

of T_1 variation in growth (Figure 1L). Quantification of *AFB4* mRNAs uncloaked a good correlation between expression levels and degree of defects in leaf shape and rosette size (Figure 1M). Evidently, petiole length became increasingly shorter in direct proportion to reduced levels of *AFB4* transcripts in antisense loss-of-function *afb4* plants (Figure 1L and 1M).

In parallel, we undertook complementation experiments through introducing *AFB4* cDNA into *afb4-1* under CaMV-35S control. Of 84 overexpression T_1 plants, we were able to place them to three groups based on leaf morphology. The majority could be classified as 35S-AFB4-H with slight but recognizable difference in leaf blade shape (Figure 1N). 35S-AFB4-M and 35S-AFB4-L consisted of nine and seven lines behaving like WT (Figure 1O) or antisense-silenced plants (Figure 1L), respectively. Two lines from each group were randomly selected for subsequent analyses of *AFB4* mRNAs. In 35S-AFB4-H, *AFB4* expression was much higher (> 10-fold) than that of WT, while the amount of *AFB4* transcripts accumulated to ~1.7-2.5-fold in 35S-AFB4-M and a much lower level in 35S-AFB4-L (Figure 1P). We further examined the number of lateral roots, the growth of leaf petioles, and the elongation of hypocotyls using *in vitro* seedlings derived from 35S-AFB4-H and 35S-AFB4-M. Apart from a narrow-spoon-like blade, slightly longer petioles were observed in 35S-AFB4-H (Figure 1Q). As expected, defects in growth and development were completely restored to WT in 35S-AFB4-M plants (Figure 1D-1J). In addition, a full restoration was also observed in soil-grown plants with respect to disease susceptibility of *afb4-1* to SCC1 (Figure 1K).

Intriguingly, we noticed that a comparable expression level to WT in several 35S lines had a similar phenotype to antisense lines. We reasoned that 35S-driven expression of *AFB4* masks cell-type specificity in transgenic lines. Actual level of *AFB4* expression in corresponding cells responsible for WT phenotype might be lower than measurement derived from rosette leaves. Intact *AFB4* locus was therefore engineered in *afb4-1* for genetic complementation. Among 38 independent lines, 23 (referred to as AFB4-AFB4-M) carried ≥ 2 functional inserts and 15 (named AFB4-AFB4-S) with one single functional insert (Supplementary information, Table S1). Surprisingly, almost all T_2 seedlings in AFB4-AFB4-M developed a WT phenotype and occasionally some individuals from each line exhibited a heterozygote-like syndrome. By contrast, all T_2 antibiotic-resistant seedlings in AFB4-AFB4-S had slightly but significantly longer petioles (Figure 1Q) with symmetrically downcurled leaves reminiscent of 35S-AFB4-H plants. To correlate this unexpected phenomenon with expression of the transgene, we quantified abundance of *AFB4* mRNAs in randomly selected plants (Supplementary information, Figure S6). Curiously, levels of *AFB4* transcripts in AFB4-AFB4-M were ~30 to 60-fold over that of WT. In AFB4-AFB4-S progeny, we found ~10 to 20-fold increase. Based on this finding, we suspect that either *cis- or trans*-regulatory elements for repression of *AFB4* expression are missing in the transgene. Conceivably, plants overexpressing moderate levels of *AFB4* mRNAs are likely to contain elevated levels of AFB4 but an extremely high concentration might trigger AFB4 protein aggregation in order to achieve a normal cellular level.

Since a high mutation frequency often occurs in TILLING lines [9, 10], *afb4-1* therefore provided an alternative tool to exclude any possible effects caused by the complicated genetic background of *afb4-2* or *afb4-3*. To this end, we raised >100 independent transgenic lines bearing *AFB4:AFB4-GUS* as described previously [1]. To our surprise, no effect was observed in these transgenic lines albeit the existence of *AFB4-GUS* fusion mRNAs was verified by cDNA sequencing and GUS activity (Supplementary information, Figure S7). We further introduced point mutations into *afb4-1* in the same way as did for *AFB4:AFB4* construct. A total of 46 and 32 independent lines were raised for *afb4-2* and *afb4-3*, respectively. A detailed analysis of insertion number, *afb4* expression, and growth phenotype clearly revealed that both transgenes behaved like *AFB4* transgene (Figure 1Q, Supplementary information, Figure S8 and Table S1). These results imply that the amino-acid residue mutations in TILLING alleles have no effect on AFB4 function. However, we cannot absolutely exclude the possibility that the mutations in *afb4-2* and *afb4-3* lead to either reduced or increased activity of AFB4. In this scenario, the outcome in transgenic lines is presumably determined by amino-acid residue mutation itself and overproduction of *afb4-2 or afb4-3* transcripts. Regardless of which hypothesis is true, the data from the previous *AFB4-GUS* complementation assay in *afb4-2* [1] should be interpreted with caution.

Taken all data together, we conclude that *afb4-1* is a null allele, thus providing an excellent tool to further investigate AFB4-controlled cellular processes. Modulation of endogenous levels of *AFB4* transcripts suggests that transcriptional regulation of *AFB4* expression might be one of central mechanisms controlling AFB4-mediated signaling. Furthermore, our results indicate a key role of AFB4 in coordinating dynamic hormone-mediated signaling pathways and in balancing growth and defense responses. Although activation of defense signaling in *afb4-1* has yet to be delineated genetically and biochemically, this finding is particularly important

because *Pectobacterium carotovorium* is the causative agent of soft-rot disease with serious damage to many economically important crops and that no direct evidence of *R*-mediated resistance to this phytopathogen has been obtained yet. Experimental materials and methods are depicted in the Supplementary information, Data S1.

Acknowledgments

We thank the Nottingham Arabidopsis Stock Centre for providing the GABI-KAT T-DNA line 068E01. This work was financially supported by the Academy of Finland, the Biocentrum of Helsinki, the University of Helsinki, and the Finnish Graduate School in Plant Biology.

Zhubing Hu[1,*], Mehmet Ali Keçeli[1,*], Maria Piisilä[1], $Jing_F$ Li[1], Mantas Survila[1], Pekka Heino[1], Günter Brader[1,2], E Tapio Palva[1], Jing Li[1]

[1]*Division of Genetics, Department of Biosciences, Faculty of Biological & Environmental Sciences, University of Helsinki, FIN-00014 Helsinki, Finland;* [2]*Austrian Institute of Technology GmbH, Bioresources, Health & Environment Department, 3430 Tulln an der Donau, Austria*

*These two authors contributed equally to this work.
Correspondence: Jing Li
Tel: +358-9-19159108; Fax: +358-9-19159079
E-mail: jing.li@helsinki.fi

References

1 Greenham K, Santner A, Castillejo C, *et al*. The AFB4 auxin receptor is a negative regulator of auxin signaling in seedlings. *Curr Biol* 2011; **21**:520-525.
2 Tsukaya H. Mechanism of leaf-shape determination. *Annu Rev Plant Biol* 2006; **57**:477-496.
3 Gray WM. Hormonal regulation of plant growth and development. *PLoS Biol* 2004; **2**:e311. doi:10.1371/journal.pbio.0020311
4 Weijers D, Jürgens G. Funneling auxin action: specificity in signal transduction. *Curr Opin Plant Biol* 2004; **7**:687-693.
5 Teale WD, Paponov IA, Palme K. Auxin in action: signalling, transport and the control of plant growth and development. *Nat Rev Mol Cell Biol* 2006; **7**:847-859.
6 Liscum E, Reed JW. Genetics of Aux/IAA and ARF action in plant growth and development. *Plant Mol Biol* 2002; **49**:387-400.
7 Gray WM, Östin A, Sandberg G, Romano CP, Estelle M. High temperature promotes auxin-mediated hypocotyl elongation in *Arabidopsis*. *Proc Natl Acad Sci USA* 1998; **95**:7197-7202.
8 Li J, Brader G, Palva ET. The WRKY70 transcription factor: a node of convergence for jasmonate-mediated and salicylate-mediated signals in plant defense. *Plant Cell* 2004; **16**:319-331.
9 Greene EA, Codomo CA, Taylor NE, *et al*. Spectrum of chemically induced mutations from a large-scale reverse-genetic screen in *Arabidopsis*. *Genetics* 2004; **164**:731-740.
10 Till BJ, Reynolds SH, Greene EA, *et al*. Large-scale discovery of induced point mutations with high-throughput TILLING. *Genome Res* 2003; **13**:524-530.

(**Supplementary information** is linked to the online version of the paper on the *Cell Research* website.)